

Simple Models and Measurements of Magnetically Induced Heating Effects in Ferromagnetic Fluids

Marc T. Thompson, *Member, IEEE*

Abstract—This paper discusses several approximate analytic techniques for calculating power dissipation and forces in ferromagnetic fluids subjected to a spatially uniform but time varying magnetic field. This power dissipation results in a rising temperature in a ferrofluid sample. Several possible heating mechanisms in magnetic fluids have been investigated, including electromagnetic and hydrodynamic processes, and a simple method for prediction of power dissipation in a sample has been developed. Experimental results are given for an induction heating problem where it is shown that the power dissipation in a sample of ferrofluid cannot be explained by induction heating of the individual suspended particles. A simple viscous drag model is introduced which shows better agreement with measured power dissipation in the sample than an eddy current model for excitation frequencies under 1 MHz.

Index Terms—Ferrofluid, induction heating, magnetic circuits, magnetic liquids, modeling.

I. INTRODUCTION

A ferrofluid is a synthetic liquid that holds small magnetic particles in a colloidal suspension, with particles held aloft by their thermal energy. When subjected to an applied magnetic field, the fluid exhibits unusual properties due to simultaneous fluid mechanic and magnetic effects. The particles are sufficiently small that the ferrofluid retains its liquid characteristics even in the presence of a magnetic field, and substantial magnetic forces can be induced which result in fluid motion.

There are three primary components in a ferrofluid [1], [2]. The carrier is the liquid element in which the magnetic particles are suspended. Most ferrofluids are either water based or oil based. The suspended material are small ferromagnetic particles such as iron oxide, on the order of 100–200 Å in diameter [3], [4]. The small size is necessary to maintain stability of the colloidal suspension, as particles significantly larger than this will precipitate. A surfactant coats the ferrofluid particles to help maintain the consistency of the colloidal suspension.

The magnetic properties of the ferrofluid are strongly dependent on particle concentration and on the properties of the applied magnetic field. With an applied field, the particles align in the direction of the field, magnetizing the fluid. The tendency for the particles to agglomerate due to magnetic

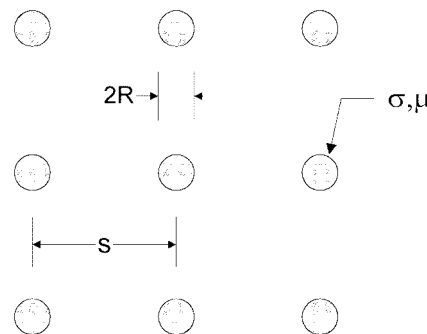


Fig. 1. Model of ferrofluid.

interactions between particles is opposed by the thermal energy of the particles. Although particles vary in shape and size distribution, insight into fluid dynamics can be gained by considering a simple spherical model of the suspended particles (Fig. 1). The particles are free to move in the carrier fluid under the influence of an applied magnetic field, but on average the particles maintain a spacing s to the nearest neighbor. In a low-density fluid, the spacing s is much larger than the mean particle radius $2R$, and magnetic dipole-dipole interactions are minimal.

Applications for ferrofluids exploit the ability to position and shape the fluid magnetically. Some applications are:

- rotary shaft seals [5], [6];
- magnetic liquid seals, to form a seal between regions of different pressures [7];
- cooling and resonance damping for loudspeaker coils [8], [9];
- printing with magnetic inks [9];
- inertial damping [10]; by adjusting the mixture of the ferrofluid, the fluid viscosity may be changed to critically damp resonances;
- accelerometers, level and attitude sensors [10], [11];
- electromagnetically triggered drug delivery [12].

To date, the hydrodynamic properties of ferrofluid have been extensively studied. However, ferrofluid heating due to magnetic induction and other effects has not been significantly studied. Heating effects in ferrofluids are important in applications where the fluid is subjected to a time varying field, as in loudspeakers where heating would adversely affect performance. Other applications exploit the ability to heat the fluid magnetically, as in the thermal actuation of a polymer gel in contact with the ferrofluid. In this study, the special case of a ferrofluid sample placed in a uniform time varying field is considered.

Manuscript received October 26, 1997.

The author was with the Laboratory for Electromagnetic and Electronic Systems, Massachusetts Institute of Technology, Watertown MA 02172 USA. He is now with the Electrical Engineering Department, Worcester Polytechnic Institute, Worcester MA USA and at 19 Commonwealth Road, Watertown, MA 02172 USA (e-mail: marcitt@mit.edu; marcitt@aol.com).

Publisher Item Identifier S 0018-9464(98)06125-1.

II. METHODS FOR POWER DISSIPATION ESTIMATION IN FERROFLUIDS

The power dissipation due to magnetic induction (eddy currents) is calculated by considering the magneto-quasistatic (MQS) form of Maxwell's equations. The MQS relationships for a conducting, uniformly permeable material are

$$\begin{aligned}\nabla \times \mathbf{H} &\approx \mathbf{J} = \sigma \mathbf{E} \\ \nabla \times \mathbf{E} &= -\frac{\partial \mathbf{B}}{\partial t} = -\mu \frac{\partial \mathbf{H}}{\partial t} \\ \nabla \cdot \mathbf{B} &= 0\end{aligned}\quad (1)$$

where the linear constitutive law $\mathbf{B} = \mu \mathbf{H}$ is used. With σ and μ taken as constants, we arrive at the magnetic diffusion equation

$$\frac{1}{\mu\sigma} \nabla^2 \mathbf{H} = \frac{\partial \mathbf{H}}{\partial t}. \quad (2)$$

The diffusion equation, with appropriate boundary conditions, is used to find the distribution of magnetic field. Ampere's law, in turn, is used to find the distribution of current density in the conductive material. In the sinusoidal steady state, the time average power dissipation in the material due to induction from the applied field is

$$\langle P \rangle = \frac{1}{2} \operatorname{Re} \left\{ \int (\mathbf{E} \cdot \mathbf{J}^*) dV \right\}. \quad (3)$$

A. Cylinder in Axial Time Varying Magnetic Field

A specific eddy current problem for which there is a closed form solution is a semi-infinite cylinder in a uniform time varying axial magnetic field [Fig. 2(a)]. The cylinder has electrical conductivity σ , magnetic permeability μ , radius R , and length l_{sample} . The time-average power dissipation is given by [13]

$$\begin{aligned}\langle P \rangle &= \frac{\pi |H_o|^2 R l_{\text{sample}}}{\sigma \delta \left[J_o \left[\left(1-j\right) \frac{R}{\delta} \right] \right]^2} \operatorname{Re} \\ &\cdot \left\{ (j-1) J_1 \left[\left(1-j\right) \frac{R}{\delta} \right] J_o \left[\left(1+j\right) \frac{R}{\delta} \right] \right\}\end{aligned}\quad (4)$$

where $\delta = \sqrt{2/\omega\mu\sigma}$ is the skin depth. The total power dissipation in the cylinder is plotted in Fig. 2(b). Of special interest is the critical frequency, when the radius of the cylinder is equal to the skin depth, or

$$f_{\text{crit}} = \frac{1}{\pi R^2 \mu \sigma}. \quad (5)$$

B. Scaling Laws

Further understanding of induction heating processes is gained by considering the limiting cases of high and low frequency excitation. In the low frequency limit where $f \ll f_{\text{crit}}$, the field inside the cylinder is not significantly perturbed from its applied value. The ϕ -directed current density is proportional to the frequency of excitation, the radial distance, and to the magnitude of the applied field, or

$$J_\phi \propto \omega r H_o. \quad (6)$$

The total time-average power dissipation in the cylinder, which is proportional to the integral of J^2 over the volume of the cylinder, is

$$\langle P_{LF} \rangle \propto (\omega H_o)^2 R^4. \quad (7)$$

In the low frequency limit, the power dissipation reduces to

$$\langle P_{LF} \rangle = \frac{1}{16} \sigma \omega^2 \mu^2 |H_o|^2 \pi R^4 l_{\text{sample}}. \quad (8)$$

At frequencies significantly higher than a critical frequency the magnetic field is effectively shielded from the inside of the cylinder by induced ϕ -directed currents. The current density is concentrated on the surface of the cylinder and may be approximated as a surface current flowing in a thin layer one skin-depth thick. As the frequency increases, the value of surface current K_s stays constant, with $|K_s| \approx |H_o|$, the value necessary to fully shield fields from the inside of the cylinder. However, as the frequency is increased, the total current, which is constant ($\approx K_s l_{\text{sample}}$), travels in a thinner and thinner layer near the surface of the cylinder due to the skin depth phenomenon. This results in a higher resistance to current flow and a corresponding higher power dissipation, with the result that for $f \gg f_{\text{crit}}$ the scaling law is

$$\langle P_{HF} \rangle \propto (H_o)^2 \sqrt{\omega}. \quad (9)$$

Or, taking the limit of the full analytic solution

$$\langle P_{HF} \rangle = \frac{1}{2} \frac{|J|^2}{\sigma} (2\pi R \delta) = \frac{|H_o|^2}{\sigma \delta} \pi R l_{\text{sample}}. \quad (10)$$

These scaling laws are useful for calculating the optimal operating frequency for a given material and geometry.

The solution for the semi-infinite cylinder in a transverse magnetic field is similar [13] in frequency profile and magnitude and will not be considered here. A spherical model shows a similar power/unit volume curve versus frequency, and results are given in the Appendix.

The small size of the ferrofluid particles (on the order of 10–200 Å in diameter) results in particles which are composed of single magnetic domains [9], [14]. Therefore, little additional power loss due to domain-domain friction is seen in the ferrofluid.

C. Viscous Drag Effects

Another possible loss mechanism in a ferrofluid is viscous drag due to motion of the ferrite particles in the fluid. To date, research has been done on the induced motion of conductive fluids (magnetohydrodynamics) [15] and of ferrofluids in a traveling or rotating magnetic field (ferrohydrodynamics) [16]–[20]. However, of special interest are cases when a ferrofluid is subjected to a uniform time varying magnetic field.

The particles in a ferrofluid are free to move, both by translation and by rotation. From electromagnetic theory, the force density acting on a material with magnetic dipole moment \mathbf{M} in a field of magnetic intensity \mathbf{H} is given by [21]

$$\mathbf{F} = \mathbf{J} \times \mathbf{B} + \mu_o (\mathbf{M} \cdot \nabla) \mathbf{H}. \quad (11)$$

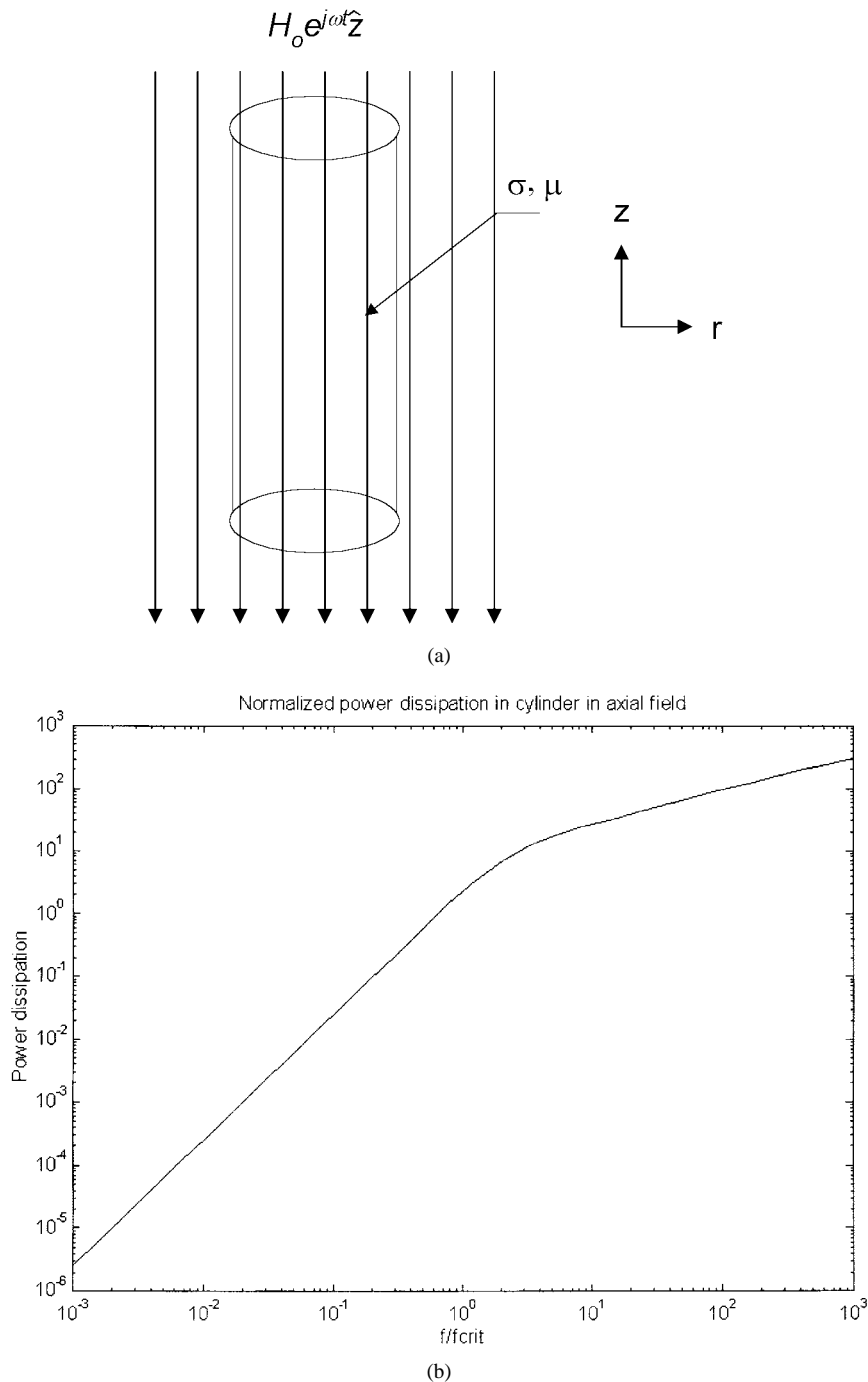


Fig. 2. Magnetically permeable conductive cylinder in uniform time varying magnetic field. (a) Geometry. (b) Solution.

In a ferrofluid, the electrical conductivity is very small [8], [11] so the Lorentz force may be neglected, resulting in

$$\mathbf{F} \approx \mu_o(\mathbf{M} \cdot \nabla)\mathbf{H}. \tag{12}$$

This is the ferrohydrodynamic force density. In magneto-hydrodynamic flows, there is a finite assumed electrical conductivity, and the Lorentz force density is the dominant effect [18]. In ferrohydrodynamic flows, a force density requires a gradient in the applied magnetic field.

The magnetic body torque density is given by [19], [20]

$$\mathbf{T} = \mu_o(\mathbf{M} \times \mathbf{H}). \tag{13}$$

For fluid rotation, the magnetization must not be collinear with the magnetic field. With magnetization effects, the magnetic flux density is defined as

$$\mathbf{B} = \mu_o(\mathbf{H} + \mathbf{M}). \tag{14}$$

In a magnetically linear material, the magnetization is given by

$$\mathbf{M} = \chi_o \mathbf{H} \tag{15}$$

where χ_o is the magnetic susceptibility.

For a ferrofluid under ac excitation, the magnetization will attempt to follow the applied field, but the fluid viscosity and Brownian motion cause the magnetization to lag the

magnetic field. The magnetization relaxation equation, with the ferrofluid undergoing simultaneous translation and rotation, is given by [20]

$$\frac{\partial \mathbf{M}}{\partial t} + (\mathbf{v} \cdot \nabla) \mathbf{M} - \left(\frac{d\Omega}{dt} \right) \times \mathbf{M} + \frac{1}{\tau} \mathbf{M} = \frac{1}{\tau} \chi_o \mathbf{H} \quad (16)$$

where v is the fluid velocity, $d\Omega/dt$ is the fluid angular velocity, and τ is the time constant associated with the magnetization process. The first three terms in the equation are the convective derivative as applied to the time rate of change of magnetization, which includes effect due to rotation and translation. In order to find the velocity and angular momentum fields, the magnetization equation must be solved self-consistently with the equations of fluid dynamics.

A special limiting case is the time varying case, with only slow rotation or translation of the ferrofluid particles, where

$$\frac{d\mathbf{M}}{dt} + \frac{1}{\tau} \mathbf{M} = \frac{1}{\tau} \chi_o \mathbf{H}. \quad (17)$$

The solution to this limiting case in the sinusoidal steady state is

$$\hat{\mathbf{M}} = \left\{ \frac{\chi_o}{j\omega\tau + 1} \right\} \hat{\mathbf{H}} \quad (18)$$

where $\hat{\mathbf{M}}$ and $\hat{\mathbf{H}}$ are complex amplitudes. This equation suggests a mechanism by which the magnetization may lag the applied magnetic field due to a time constant in the magnetic susceptibility, resulting in a time varying torque which causes rotation of a ferrofluid particle.

In a low frequency field, it has been theorized that the particles are alternately oriented in one or the other directions, depending on the direction of the excitation field [4]. If the frequency is raised, the viscous drag force (proportional to particle angular velocity) becomes more important.

D. Viscous Drag on a Rotating Sphere in a Fluid

The total viscous drag force on a rigid sphere immersed in a fluid is easily calculated if the Reynolds number is low. For fluid flow, the Reynolds number is given by

$$R_y = \frac{\rho_f U L}{\eta} \quad (19)$$

where ρ_f is fluid density, U is the magnitude of the fluid velocity, l is the length scale of the flow over the surface, and η is the viscosity. This number is the ratio of an inertial force density to a viscous force density. Therefore, for low Reynolds number flows, viscous forces dominate. Due to the small size of ferrofluid particles, low Reynolds flows are expected.

The torque acting on a sphere rotating in a stationary fluid is given by [23], [24]

$$T_d \approx 8\pi\eta R^3 \dot{\theta} \approx c_t \dot{\theta} \quad (20)$$

where c_t is the torsional damping coefficient.

E. Estimation of Power Loss Due to Particle Rotation

In a uniform magnetic field, there is no net force acting on the particle, even if there is a time lag between the magnetic field and the particle magnetization [19]. However, there is a time varying torque if the field and magnetization are not collinear.

The torsional motion of the particle obeys the equation of motion

$$I_\theta \ddot{\theta} + c_t \dot{\theta} + k_t \theta = T(t), \quad (21)$$

In the case of the ferrofluid, where we assume that there are no dipole-dipole interactions between magnetized particles, we take the torsional spring constant to be $k_t = 0$. The equation of motion may be reduced to a first-order equation in angular velocity ($\Omega = \dot{\theta}$) as

$$\frac{d\Omega}{dt} + \frac{c_t}{I_\theta} \Omega = \frac{T(t)}{I_\theta}. \quad (22)$$

For the sphere of mass M and density ρ , the mass moment of inertia is given by [25]

$$I_\theta = \frac{2}{5} MR^2. \quad (23)$$

The factor I_θ/c_t may be taken as a time constant, which is related to the relaxation of the magnetization. With an iron particle of radius $R = 10^{-8}$ m, density $\rho_{FE} = 7.8 \times 10^9$ kg/m³, in a water based ferrofluid with $\eta = 10^{-3}$ kg/m-s, the computed time constant is

$$\tau_{\text{slow}} = \frac{I_\theta}{c_t} = \frac{\frac{2}{5} MR^2}{8\pi\eta R^3} = \frac{\rho_{FE} R^2}{15\eta} \approx 53 \mu\text{s}. \quad (24)$$

This is a plausible result, based on the reported ranges of magnetization time constants reported in the literature [14], [26] and the numerous simplifying assumptions in this calculation. However, it is likely still to be a gross approximation, as it has been shown that the viscosity of a ferrofluid varies considerably with particle concentration and applied magnetic field [1].

The slow component of magnetization is fixed to the rotating magnetic particle (Fig. 3). The torque on the sphere is time varying due to time variations in the applied magnetic field [17] and due to spatial variations, or

$$T(\theta, t) = \mu_o m(t) H(t) \sin \theta. \quad (25)$$

The magnetic dipole moment for a fully magnetized sphere comprised of magnetically permeable material with $\mu \gg \mu_o$ is [21]

$$m \approx 4\pi R^3 H_o. \quad (26)$$

This number may be taken as an upper bound for the magnitude of the magnetization vector, as particle rotation will also affect the actual value of magnetization.

For low frequency excitation, the nonlinear differential equation relating angular velocity to torque predicts a power

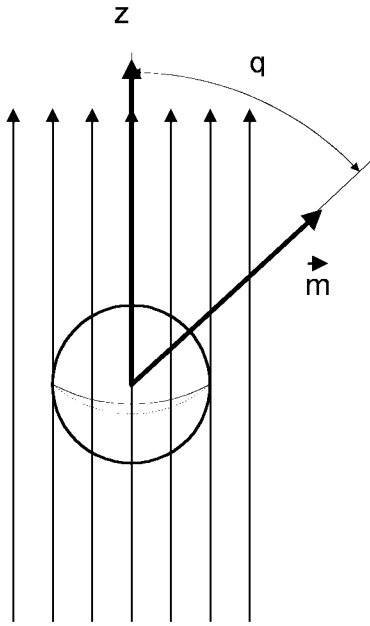


Fig. 3. Model of magnetized ferrofluid particle in applied field.

dissipation that increases approximately linearly with frequency. The mechanism is as follows.

- When the magnetic field changes polarity, the torque on the magnetic particle tends to orient the particle with its magnetization vector in the direction of the applied field.
- If the frequency of excitation is lower than the inverse of the relaxation time τ_{slow} , the particle will rotate fully so that it is oriented with the field. The rotation results in an instantaneous power dissipation due to viscous drag.
- The particle remains stationary, oriented with the field, until the polarity of the applied field changes sign.
- If the field excitation frequency is increased, the number of particle rotations per second increases, resulting in higher power dissipation.

For low frequency excitation, the angular velocity may be approximated by

$$\dot{\theta} \approx \frac{T(t)}{c_t} \quad (27)$$

where the inertia of the particle has been ignored. This approximation holds if the acceleration forces are small compared to the viscous drag force or if $|I_\theta \ddot{\theta}| \ll |c_t \dot{\theta}|$. In this case the model reduces to one which is time varying, but whose solution is essentially static. As a gross estimation, the torque is approximated by one-quarter of the maximum value, since this is the average value of the $\sin^2(\omega t)$ function multiplied by the factor of half which accounts for the fast component of magnetization. Therefore, the estimate for average torque is

$$T(\theta, t) = T_o \approx \pi \mu_o R^3 H_o^2. \quad (28)$$

The work done in rotating a particle an angle θ degrees is $T_o \theta$ if the torque is constant; the average power dissipation in rotating a particle 180° at a frequency f is

$$\langle P \rangle = 2\pi T_o f \quad (29)$$

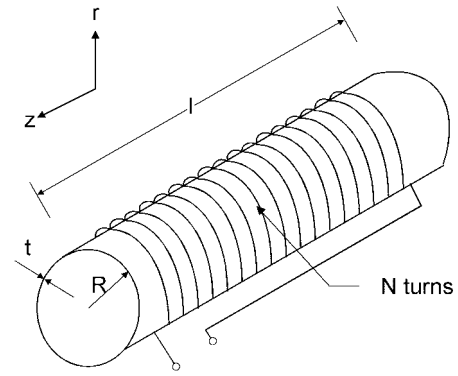


Fig. 4. Test coil geometry.

where there is a factor of two because there are two particle rotations per electrical cycle. Using this approximation, the total power dissipation in the ferrofluid sample due to rotation of the spheres is

$$\langle P \rangle \approx 2N_{\text{particles}} \pi T_o f \approx 2N_{\text{particles}} \pi^2 \mu_o R^3 H_o^2 f \quad (30)$$

where $N_{\text{particles}}$ is the total number of rotating fluid particles in the sample, and the previous approximation for torque was used. Assuming a constant torque, the model has limited validity for magnetic excitation frequencies

$$\omega < \dot{\theta}. \quad (31)$$

For expected value of torque and damping coefficient ($c_t \approx 2.5 \times 10^{-26}$ N-m-s, $T_o = 2.6 \times 10^{-22}$ N-m for a field of $H_o = 1400$ A/m) the range of validity is approximately $\omega < 10000$ rad/s. This simple expression assumes low frequency operation, with time scales slow as compared to the slow magnetization relaxation time, and neglects dipole/dipole interactions. Furthermore, particle inertia is ignored, due to the small size of the particles. For higher frequency operation, the full ferrohydrodynamic equations must be solved to account for the effects of particle rotation on magnetization [20].

III. EXPERIMENTS

The goal of the experiments were to make order-of-magnitude predictions of time-average power dissipation in a sample of ferrofluid under excitation by a time varying magnetic field. Calorimetric measurements have been used in to measure power dissipation [27]; however, this method requires an insulated vessel for adiabatic heating of the sample, or errors result due to conductive, convective, and radiative heat transfer. A simpler method has been developed in an experimental setup by which the change in complex terminal impedance of an air-core solenoidal inductor is measured when a sample of ferrofluid is placed inside the solenoid bore. Power dissipation in the sample as a function of frequency is calculated based on the measured impedance change. This impedance is due in part to the induced power dissipation in the ferrofluid.

An experimental solenoidal coil was constructed for the purposes of measuring the electrical resistance of a sample of ferrofluid for various excitation frequencies. A solenoid

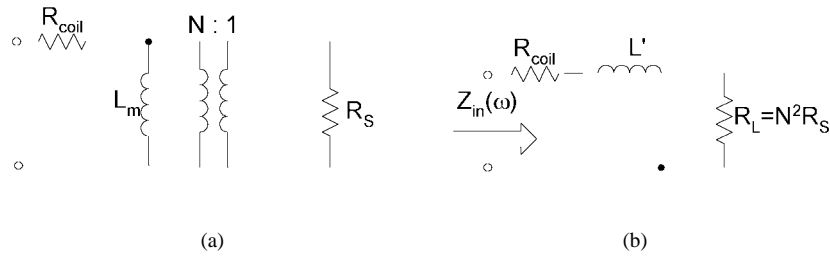


Fig. 5. Lumped circuit model of induction heating problem.

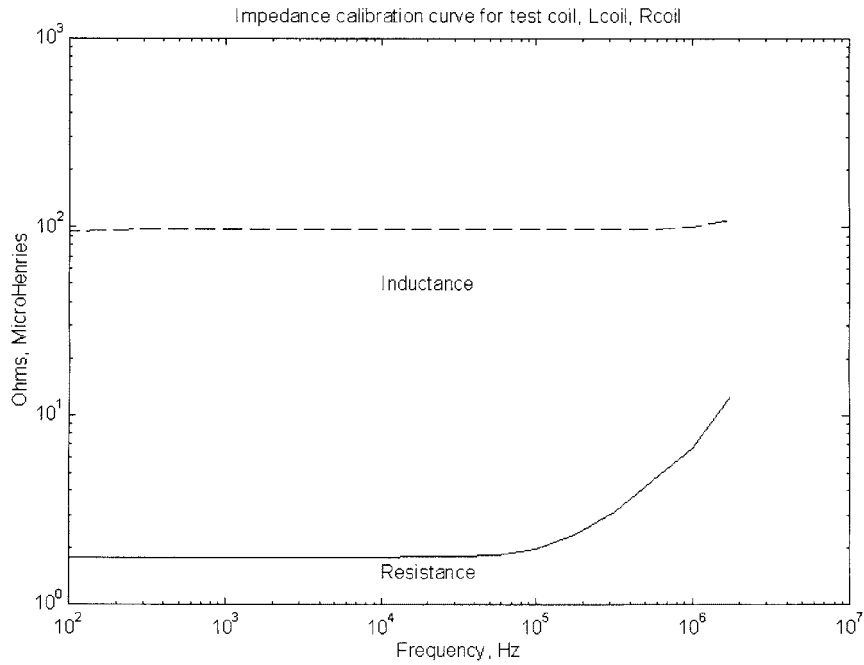


Fig. 6. Test coil calibration curve, measurement of L_{coil} , R_{coil} with empty solenoid bore.

was constructed with 150 turns of #30 gauge wire uniformly wrapped on a plastic cylindrical winding form. For the long solenoidal coil (Fig. 4) with $2b \gg R$ and $R \gg t$, the field inside the coil is uniform and z-directed, with a magnitude given by

$$H_o \approx \frac{NI_o}{2b} \quad (32)$$

where I_o is the magnitude of the excitation current source.

The solenoid coil acts as a transformer, and the conductive insert acts as a shorted transformer secondary with resistance R_w (Fig. 5). R_{coil} is the resistance of the primary test coil, which changes with frequency (due to skin and proximity effects) and temperature. L_m is the magnetizing inductance of the primary coil, and R_s is the effective resistance of the insert. In this simple model, the leakage inductance has been ignored. With the load reflected to the primary side, and the inductance rearranged, the equivalent circuit of Fig. 6(b) results. For a reactive load driven by a current source in the sinusoidal steady state, the time average power dissipation in the insert is given by

$$\langle P_{diss} \rangle = \frac{I_o^2}{2} \text{Re}\{Z_{in}^*\} = \frac{I_o^2}{2} R_p \quad (33)$$

where R_p is the effective resistance of the insert in the solenoid bore. A Hewlett-Packard 4192A impedance analyzer was used to measure the terminal resistance as a function of frequency of a solenoidal coil loaded with electrically conductive materials. The analyzer measures the series resistance and inductance at the coil terminals, as in this model. If the change in coil resistance R_{coil} with frequency is known, then an approximation for the load resistance R_p can be calculated.

An advantage of the lumped-parameter transformer model is that it is completely general, and only the field profile inside the solenoid needs to be known in order to measure power dissipation. Therefore, the method may be easily applied to different coil and conductive insert geometries.

A. Experimental Setup and Calibration

For purposes of calibrating the test, the impedance of the coil alone as a function of frequency was first measured as a function of frequency. Fig. 6 shows the measured resistance of the test coil. The dc resistance of the coil is approximately 1.8Ω and increases above 100 kHz due to skin depth limiting in the winding wire. The low frequency inductance of the test coil is approximately $97 \mu\text{H}$ and stays constant out to approximately 1 MHz, where the self-resonant frequency of

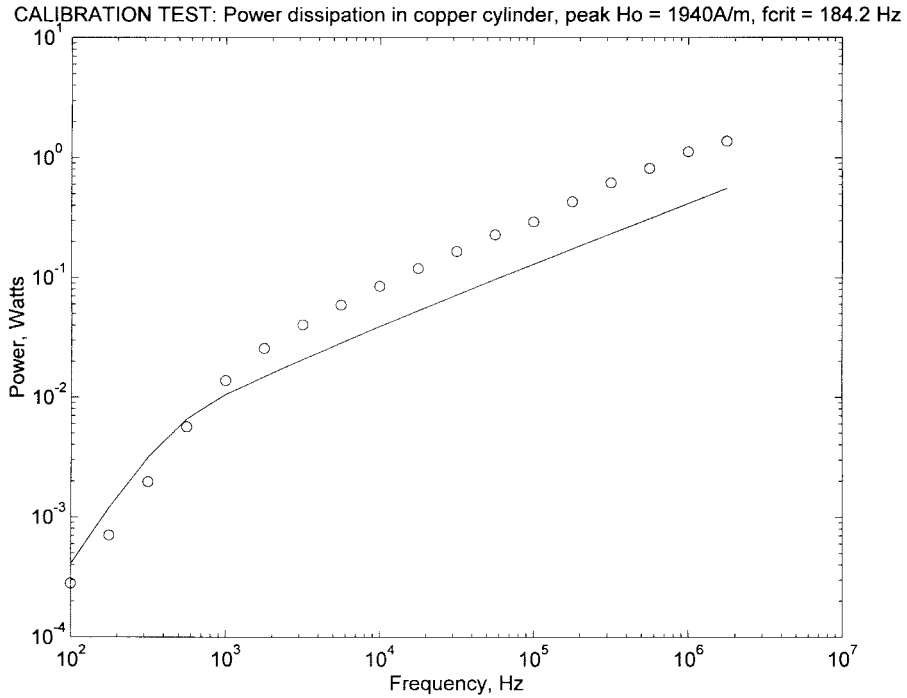


Fig. 7. Measurements on test coil, loaded with cylindrical aluminum insert. Dots: Test data based on resistance measurements on cylindrical insert. Solid line: analytical approximation based on infinitely long solenoid model.

TABLE I
SOLENOID CALIBRATION TEST PARAMETERS

Test coil cross sectional area	$A_s = 2.14 \times 10^{-4} \text{ m}^2$
Number of turns in test coil	$N = 150$
Length of test coil	$2b = 0.058 \text{ m}$
Radius of aluminum test sample	$R = 0.00625 \text{ m}$
Length of aluminum test sample	$l_{\text{sample}} = 0.017 \text{ m}$
Measured DC coil resistance	$R_{\text{coil,DC}} \approx 1.79 \Omega$
Measured low frequency series inductance	$L_{\text{LF}} = 97 \mu\text{H}$
Electrical conductivity of aluminum	$\sigma_{\text{Al}} = 3.5 \times 10^7 (\Omega\text{m})^{-1}$

TABLE II
MATERIAL PARAMETERS OF FERROFLUID

Sample volume	$1.7 \times 10^{-6} \text{ m}^3$
Electrical conductivity of particles	$\sigma_f = 3 \times 10^6 (\Omega\text{m})^{-1}$
Electrical conductivity of ferrofluid	$\sigma_{\text{fluid}} < 10^{-7} (\Omega\text{m})^{-1}$ [5]
Volume percentage of particles	$\approx 3\%$ by volume [5]
Initial magnetic permeability of particles	$\mu \approx 100 \mu_0$ [5]
Particle mean radius	$R \approx 10^{-8} \text{ m}$
Density of magnetite particles	$\rho_{\text{FE}} = 7.8 \text{ g/cm}^3$
Fluid density	$\rho_f = 1 \text{ g/cm}^3$
Fluid viscosity of carrier fluid	$\eta = 1 \text{ cp} = 0.01 \text{ g/cm-sec}$

the coil is approached. This data was used in later tests in order to approximate the resistive load due to the conductive insert.

The terminal resistance was then tested with an aluminum cylinder insert resulting in a measured terminal resistance R_{meas} . Test parameters of the experimental solenoid and aluminum sample are shown in Table I. After subtracting the measured coil resistance, the load resistance due the aluminum

is found by $R_P(\omega) = R_{\text{meas}}(\omega) - R_{\text{coil}}(\omega)$. As the aluminum was inserted into the solenoid bore, the measured terminal resistance increased due to power dissipation in the aluminum, with the power dissipation in the aluminum calculated by

$$\langle P_{\text{diss}}(\omega) \rangle = \frac{I_0^2}{2} R_P(\omega), \quad (34)$$

$$\langle P_{\text{diss}} \rangle = \frac{3\pi R^5 \omega^2 \mu^2 (\mu_0 H_0)^2 \sigma \left\{ \frac{1}{2} u(S+s) - C + c \right\}}{(\mu - \mu_0)^2 \{ (pR^2 + 1)C + (pR^2 - 1)c - u(S+s) \} + (\mu - \mu_0) pR^2 u(S-s) + p^2 R^4 (C-c)}$$

$$u = R\sqrt{2p} = \frac{2R}{\delta}$$

$$p = \omega\mu\sigma = \frac{2}{\delta^2}$$

$$C = \cosh u$$

$$c = \cos u$$

$$S = \sinh u$$

$$s = \sin u.$$

(35)

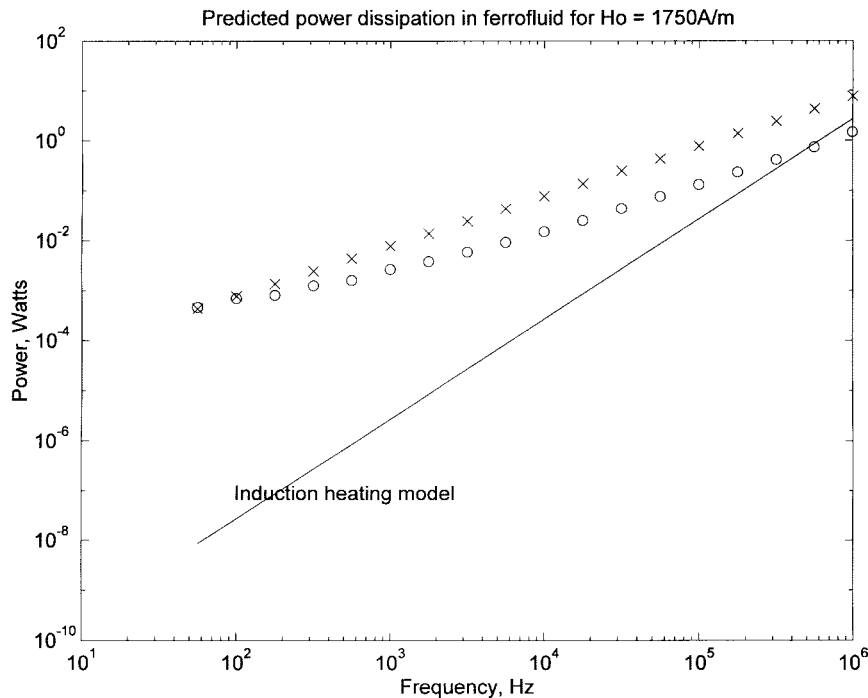


Fig. 8. Predicted power dissipation in ferrofluid. Solid line—prediction based on induction heating only. Dots: results from measurements on ferrofluid. xxx: predictions based on low frequency viscous drag model.

The oscillator voltage level was set to 1.0 V p-p, resulting in a calculated low frequency field inside the solenoid bore of approximately 1400 A/m. This corresponds to a magnetic flux density B_o of approximately 180 Gauss, which is less than the expected saturation magnetization of the ferrofluid.

Assuming that the field profile inside the solenoid is uniform, the power dissipation in the aluminum may be calculated analytically by substituting for H_o in terms of I_o , as given earlier, $H_o = NI_o/(2b)$. Using this formula, the measurement based on resistance measurement is compared to the time average power calculated using the analytic solution for the semi-infinite solenoid (Fig. 7). The results show fair match of the predicted and measured curves, with differences attributable to end effects in the solenoid and cylindrical insert, since the analytic solution assumes an infinitely long solenoid and insert. This shows that the impedance measurement technique will give useful order-of-magnitude estimates for power dissipation in the sample of ferrofluid.

B. Experimental Results with Ferrofluid

A sample of water-based ferrofluid was prepared and placed in the center of the solenoid bore. Material parameters of the ferrofluid sample are shown in Table II. The terminal resistance change at the solenoid terminals was measured and a resulting power dissipation was calculated for a field strength of $H_o = 1400$ A/m. Care was taken to calibrate the test for changes in operating frequency and temperature dependence of the coil resistance. The data shows that the ferrofluid loss over the 100 Hz–1 MHz frequency range varies approximately with frequency.

The predicted power dissipation in the sample of ferrofluid is plotted in Fig. 8 and compared to the predicted power

dissipation if the only loss mechanism were induction heating of the individual ferrofluid particles. In the induction heating calculation, semi-infinite cylinders are considered for ease of calculation. It can be shown that the solution for spherical models is of similar magnitude and frequency profile. The resulting plot shows that the component of power loss due to eddy currents has an ω^2 dependence for frequencies under 1 MHz, due to the small size of the particles. Furthermore, there is a several order of magnitude difference between the measured power dissipation and the predicted power dissipation based on electromagnetic induction only in this frequency range. Therefore, it is likely that induction heating is not the dominant heating effect for these frequencies.

Results are also plotted on the same graph for the viscous drag model discussed earlier. The power dissipation using the simple viscous drag model has approximately the same frequency dependence as the measured data. The fact that the measured power in the ferrofluid is higher than predicted by the simple model may indicate that there are also viscous drag forces present due to a finite fluid velocity field due to nonuniformities in the field of the solenoid bore. Also, the model presented is valid to approximately $1/\tau_{\text{slow}}$, which for the fluid considered is approximately 20 kHz. A more complicated ferrohydrodynamic model is needed for higher frequencies.

IV. CONCLUSIONS

Results of impedance measurements on a sample of ferrofluid show a linear dependence of power loss versus excitation frequency in the 100 Hz–1 MHz range, results that are unexplained by normal induction-heating methods alone. It has been shown that the data can be fit to a model which is

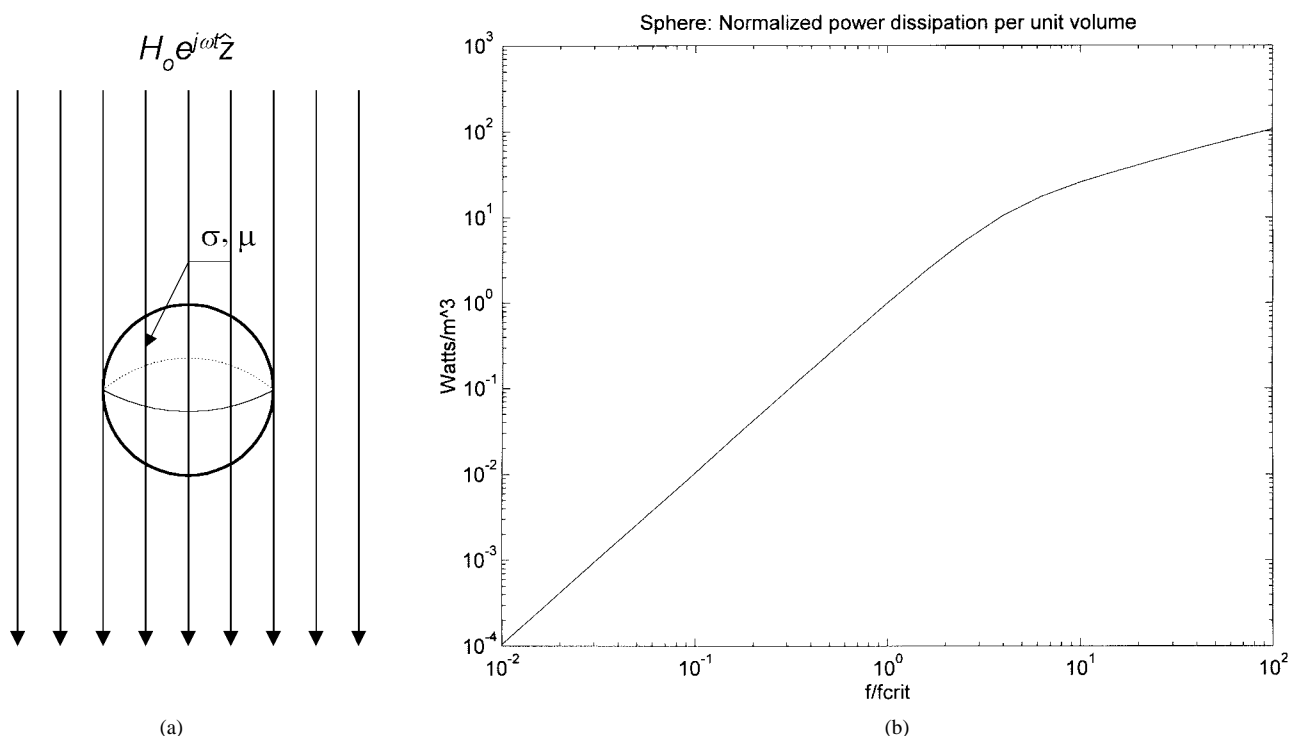


Fig. 9. Magnetically permeable conductive sphere in uniform time varying magnetic field. (a) Geometry. (b) Analytic solution for sphere problem.

consistent with the theories of magnetic fluid particle rotation in a uniform magnetic field caused by a time lag between the applied field and the induced particle magnetization. This theory could be further tested by repeating the experiments with a sample of frozen ferrofluid, where no particle motion would be allowed. In that case, the expected power dissipation in the sample would be much less over a wide frequency range.

The model used did not take into account the possibility of dipole-dipole interactions in the ferrofluid [28], [29]. Magnetic interactions may induce particle clumping, which would affect the loss mechanisms significantly. The dipole interaction problem in ferrofluids is not yet well understood and is an active area of research [4], [14], [28], [29].

Sources of error in the measurements are introduced due to the finite extent of the solenoid, leakage inductance which causes a modification of the field inside the solenoid, the uncertainties in the properties of the ferrofluid (such as particle size, density, variation of viscosity with magnetic field [30], and saturation magnetization), and the simplicity of the ferrohydrodynamic model used. The simple hydrodynamic model presented could be modified, and nonlinear simulations run to account for the time varying torque due to the rotation of the ferrofluid particle. It is likely that in addition to the particle spinning that there is a velocity field which adds additional power dissipation, due to gradients in the field inside the finite solenoid. The tests could be repeated with a larger solenoid with a higher length/diameter ratio and a test sample which is small in width compared to the diameter of the solenoid bore.

APPENDIX

The solution for the power dissipation in the conducting sphere in a uniform time varying field [Fig. 9(a)] involve

modified Bessel functions of order 1/2 and 3/2. The solution, given in Smythe [31], is shown in (35) located at the bottom of the second previous page.

The solution is plotted in Fig. 9(b), which shows a quadratic dependence on power loss below the critical frequency, and a square-root dependence above the critical frequency. This plot is similar to and consistent with the earlier analysis done on a conductive cylinder.

ACKNOWLEDGMENT

The author would like to thank Prof. S. Leeb and Prof. R. Thornton of the Massachusetts Institute of Technology for helpful discussions, and D. Megna, who assisted in performing the experiments.

REFERENCES

- [1] R. Kaiser and L. G. Miskolczy, "Some applications of ferrofluid magnetic colloids," *IEEE Trans. Magn.*, vol. MAG-06, pp. 694–698, Sept. 1979.
- [2] K. Raj and B. Moskowitz, "Ferrofluids step up motor precision," *Mach. Des.*, pp. 57–60, Jan. 26, 1995.
- [3] R. Chantrell, J. Popplewell, and S. Charles, "Measurements of particle size distribution parameters in ferrofluids," *IEEE Trans. Magn.*, vol. MAG-14, pp. 975–977, Sept. 1978.
- [4] P. Scholten, "Magnetic measurements on particles in suspension," *IEEE Trans. Magn.*, vol. MAG-11, pp. 1400–1402, Sept. 1975.
- [5] Z. Jibin and L. Yongping, "Numerical calculations for ferrofluid seals," *IEEE Trans. Magn.*, vol. 28, pp. 3367–3371, Nov. 1992.
- [6] R. Moskowitz and E. D. Torre, "Hysteretic magnetic dipole interaction model," *IEEE Trans. Magn.*, vol. MAG-3, pp. 579–586, Dec. 1967.
- [7] M. Perry and T. B. Jones, "Hydrostatic loading of magnetic liquid seals," *IEEE Trans. Magn.*, vol. MAG-12, pp. 798–800, Nov. 1976.
- [8] *Ferrofluid APG047 specification sheet*, Ferrofluidics Corp, Nashua, NH, 1992.
- [9] J. Popplewell and S. W. Charles, "Ferromagnetic Fluids—Their magnetic properties and applications," *IEEE Trans. Magn.*, vol. MAG-17, no. 6, pp. 2923–2928, Nov. 1981.

- [10] Bailey, "Lesser known applications of ferrofluids," *J. Magnetism Magn. Mater.*, vol. 39, pp. 178-182, 1983.
- [11] Y. Kanamaru, T. Fumino, J. Kanamoto, and S. Notsu, "Characteristics of level and two axis attitude detector using magnetic fluid," *IEEE Trans. Magn.*, vol. MAG-23, pp. 2203-2205, Sept. 1987.
- [12] E. C. Lupton, X. Yu, S. B. Leeb, and G. Hovorka, "Electromagnetically triggered, responsive gel based drug delivery device," U.S. Patent application, Feb. 24, 1995.
- [13] M. Zahn, "Power dissipation and magnetic forces in MAGLEV rebars," Internal Rep., Laboratory for Electromagnetic and Electronic Systems, 1995.
- [14] C. Sanchez, J. Gonzalez-Miranda, and J. Tejada, "Computer simulation of slow magnetic relaxation," *J. Magnetism Magn. Mater.*, vols. 140-144, pp. 365-366, 1995.
- [15] A. Kulikovskiy and G. Lyubimov, *Magnetohydrodynamics*. Reading, MA: Addison-Wesley, 1965.
- [16] J. Bacri, A. Cebers, S. Lacis, and R. Perzynski, "Dynamics of a magnetic fluid droplet in a rotating field," *J. Magnetism Magn. Mater.*, vol. 149, pp. 143-147, 1995.
- [17] R. Moskowitz, "Ferrofluids: liquid magnetics," *IEEE Spectrum*, pp. 53-57, Mar. 1975.
- [18] J. Neuringer and R. Rosensweig, "Ferrohydrodynamics," *Phys. Fluids*, vol. 7, no. 12, pp. 1927-1937, Dec. 1964.
- [19] M. Zahn, "Ferrohydrodynamic Torque-Driven Flows," *J. Magnetism Magn. Mater.*, vol. 85, pp. 181-186, 1990.
- [20] M. Zahn and D. Greer, "Ferrohydrodynamic pumping in spatially uniform sinusoidally time varying magnetic fields," *J. Magnetism Magn. Mater.*, vol. 149, pp. 165-173, 1995.
- [21] H. Haus and J. Melcher, *Electromagnetic Fields and Energy*. Englewood Cliffs, NJ: Prentice-Hall, 1989.
- [22] G. Kronkalns, "Measuring the thermal conductivity and the electrical conductivity of a ferrofluid in a magnetic field," *Magnetohydrodynamics*.
- [23] L. Landau and E. Lifshitz, *Fluid Mechanics*, 2nd ed. Oxford, U.K.: Pergamon Press, 1987, p. 91.
- [24] P. Stiles and M. Kagan, "Frictional torque on an ellipsoid rotating in a uniformly magnetized ferrofluid," *J. Colloid Interface Sci.*, vol. 125, no. 2, pp. 493-496, Oct. 1988.
- [25] J. Williams, *Fundamentals of Applied Dynamics*. New York: Wiley, 1996, p. 289.
- [26] B. Matygullin, "Drag on a sphere containing a ferromagnetic suspension in a rotating magnetic field," *Mgnehdrodynamics*, no. 3, pp. 136-138, July-Sept. 1976.
- [27] S. Leeb, private communication, Massachusetts Institute of Technology, 1996.
- [28] R. Moskowitz and R. Rosensweig, "Nonmechanical torque-driven flow of a ferromagnetic fluid by an electromagnetic field," *Appl. Phys. Lett.*, vol. 11, no. 10, pp. 301-303, Nov. 15, 1967.
- [29] R. Moskowitz and E. D. Torre, "Computer simulation of the magnetic dipole interaction problem," *J. Appl. Phys.*, vol. 38, no. 3, pp. 1007-1009, Mar. 1967.
- [30] R. Rosensweig, R. Kaiser, and G. Miskolczy, "Viscosity of magnetic fluid in a magnetic field," *J. Colloid Interface Sci.*, vol. 29, no. 4, pp. 680-686, Apr. 1969.
- [31] W. Smythe, *Static and Dynamic Electricity*, 2nd ed. New York: McGraw Hill, 1950, p. 400.

Marc T. Thompson (M'92) received the B.S.E.E. degree from the Massachusetts Institute of Technology (MIT), Cambridge, MA, in 1985, the M.S.E.E. degree in 1992, the electrical engineer's degree in 1994, and the Ph.D. degree in 1997.

His research areas at MIT included other topics such as: analysis of heating effects in magnetic fluids, and electromechanical stability analysis of magnetic structures. His doctoral thesis at MIT, "High Temperature Superconducting Magnetic Suspension for Maglev," concerned the design and test of high-temperature superconducting suspensions for MAGLEV and the implementation of magnetically-based ride quality control. Currently, he is an Engineering Consultant and Adjunct Associate Professor of Electrical Engineering at Worcester Polytechnic Institute (W.P.I.), Worcester, MA. He has worked as a consultant in analog, electromechanics, and magnetics design, and holds two patents. At W.P.I. he teaches intuitive methods for analog circuit and power electronics design, and currently works as a consultant for Magnemotion, Inc., Thornton Associates, Inc., and Polaroid Corporation.